Megakaryocyte-restricted *MYH9* inactivation dramatically affects hemostasis while preserving platelet aggregation and secretion

Catherine Léon,[1-3] Anita Eckly,[1-3] Béatrice Hechler,[1-3] Boris Aleil,[1-3] Monique Freund,[1-3] Catherine Ravanat,[1-3] Marie Jourdain,[1-3] Christelle Nonne,[1-3] Josiane Weber,[1-3] Ralph Tiedt,[4] Marie-Pierre Gratacap,[5,6] Sonia Severin,[5,6] Jean-Pierre Cazenave,[1-3] François Lanza,[1-3] Radek Skoda,[4] and Christian Gachet[1-3]

[1]INSERM, U311 Strasbourg, France; [2]Établissement Français du Sang–Alsace, Strasbourg, UMR-S311 France; [3]Université Louis Pasteur, Strasbourg, UMR-S311 France; [4]Department of Research, Experimental Hematology, University Hospital Basel, Basel, Switzerland; [5]Institut National de la Santé et de la Recherche Médicale, U563 Centre de Physiopathologie de Toulouse, Département d'Oncogenèse et Signalisation dans les Cellules Hématopoïétiques, Toulouse, France; [6]Université Toulouse III Paul Sabatier, Faculté de médecine Toulouse-Purpan, UMR-S563, Toulouse, France

Mutations in the *MYH9* gene encoding the nonmuscle myosin heavy chain IIA result in bleeding disorders characterized by a macrothrombocytopenia. To understand the role of myosin in normal platelet functions and in pathology, we generated mice with disruption of *MYH9* in megakaryocytes. *MYH9*Δ mice displayed macrothrombocytopenia with a strong increase in bleeding time and absence of clot retraction. However, platelet aggregation and secretion in response to any agonist were near normal despite absence of initial platelet contraction. By contrast, integrin outside-in signaling was impaired, as observed by a decrease in integrin β3 phosphorylation and PtdIns(3,4)P_2 accumulation following stimulation. Upon adhesion on a fibrinogen-coated surface, *MYH9*Δ platelets were still able to extend lamellipodia but without stress fiber–like formation. As a consequence, thrombus growth and organization, investigated under flow by perfusing whole blood over collagen, were strongly impaired. Thrombus stability was also decreased in vivo in a model of $FeCl_3$-induced injury of carotid arteries. Overall, these results demonstrate that while myosin seems dispensable for aggregation and secretion in suspension, it plays a key role in platelet contractile phenomena and outside-in signaling. These roles of myosin in platelet functions, in addition to thrombocytopenia, account for the strong hemostatic defects observed in *MYH9*Δ mice. (Blood. 2007;110:3183-3191)

Introduction

Important morphologic changes occur in platelets during their activation at sites of vascular injury. The cells lose their resting discoid shape to become spheroid and contracted, emitting membrane blebs and longer extensions.[1-4] Once in contact with a surface, the spheroid platelets extend long filopodia and finally spread over it by emitting thin, sheet-like lamellipodia.[1,2] Myosin activation plays a central role in the cytoskeletal rearrangements underlying these changes in morphology. Myosin becomes activated after phosphorylation of the myosin regulatory light chain (RLC), which results from both calcium-regulated myosin light-chain kinase activity and Rho kinase–regulated myosin phosphatase activity.[5-8] Activated myosin assembles into short filaments through the myosin heavy chain and interacts mainly with central actin filaments. Myosin has been proposed to participate in several platelet contractile functions such as platelet spheration, contraction and stress-fiber formation, and fibrin clot retraction. Platelet spheration and contraction, as observed in the aggregometer, closely correlate with phosphorylation of the RLC[9,10] and are prevented when RLC phosphorylation is inhibited.[6,7,9,10] Myosin has also been shown to be associated with stress fiber–like structures in spreading adherent platelets.[11] In addition, myosin could play a role in platelet secretion, as it is decreased by inhibition of myosin RLC phosphorylation.[5,12-15] Finally, a role of myosin in clot retraction has long been suspected in view of the necessity for a contractile force and was recently confirmed using a direct inhibitor of myosin activity.[16]

Several of these platelet functions are altered in patients carrying mutations in the *MYH9* gene encoding the nonmuscle myosin heavy chain IIA (NMHC-IIA), which is the only myosin heavy-chain isoform present in platelets.[17] Mutations in this gene are responsible for the so-called *MYH9*-related disorders, which encompass several autosomal-dominant diseases previously classified as May-Hegglin anomaly, Fechtner syndrome, Sebastian syndrome, or Epstein syndrome.[18-20] Different mutations have been reported that in all cases result in abnormal NMHC-IIA. All of these patients share the triad of thrombocytopenia, large platelets, and characteristic leukocyte inclusions (Döhle-like bodies) composed of ribosomes, endoplasmic reticulum, and abnormal myosin aggregates.[21,22] Platelets from these patients fail to undergo shape change in the aggregometer in response to agonists but display normal aggregation.[18,23-25] While most patients are asymptomatic or have a mild bleeding tendency, a few suffer from significant bleeding either spontaneously or during childbirth or surgical procedures.[26] Other manifestations may occur such as cataracts, sensorineural deafness, or nephritis, which is consistent with the wide tissue expression of NMHC-IIA. Most of these other manifestations appear later during adulthood, probably because of the presence of other heavy-chain isoforms in the tissues involved that

Submitted March 14, 2007; accepted July 20, 2007. Prepublished online as *Blood* First Edition paper, July 30, 2007; DOI 10.1182/blood-2007-03-080184.

An Inside *Blood* analysis of this article appears at the front of this issue.

The online version of this article contains a data supplement.

The publication costs of this article were defrayed in part by page charge payment. Therefore, and solely to indicate this fact, this article is hereby marked "advertisement" in accordance with 18 USC section 1734.

compensate for the abnormal NMHC-IIA.[20,27,28] The molecular mechanisms leading to the platelet abnormalities are still subject to debate. Some studies suggested that mutations in *MYH9* led to a dominant-negative effect, "poisoning" the wild-type myosin.[21,29] Others showed that the disease resulted from a haploinsufficiency,[30] and a more recent study suggested haploinsufficiency in the megakaryocytic lineage associated with a dominant-negative effect in granulocytes.[31]

To explore the role of myosin and the effects of myosin deficiency on the hemostatic functions of platelets, we generated mice with disruption of *MYH9*. Since previous studies have shown early embryonic mortality in *MYH9*$^{-/-}$ mice[28,32] (C.L., September 2005, unpublished data), we used the loxP-Cre system to restrict the *MYH9* knock out to the megakaryocyte lineage. Mice carrying a floxed *MYH9* first exon were crossed with transgenic mice carrying cre-recombinase under the regulation of the platelet PF4 promoter.[33] Inactivation of *MYH9* in megakaryocytes resulted in a severe defect in platelet myosin expression with a phenotype resembling that of *MYH9*-related diseases, including thrombocytopenia, large and immature platelets, and impaired platelet contractile activity. Our data show that whereas platelet aggregation and secretion responses were only moderately affected, myosin deficiency led to dramatically disturbed primary hemostasis with severely prolonged tail bleeding times and a total absence of clot retraction. The platelet contractile shape change and outside-in signaling were affected, inhibiting thrombus growth in vitro under flow and in vivo following vessel wall injury.

Materials and methods

Materials

Equine tendon collagen was from Nycomed (Munich, Germany) and human fibrinogen from Kabi (Uppsala, Sweden). BSA, busulfan, thrombin, and anti–NMHC-IIA antibody were from Sigma-Aldrich (St Quentin Fallavier, France). Blebbistatin was from Calbiochem (VWR, Meudon, France). Eptifibatid was from GlaxoSmithKline, Greenford, United Kingdom. Jon/A-PE antibody, FITC-labeled antifibrinogen antibody, anti-CD41/CD61-PE, and anti-CD61 (β3 integrin) antibodies were from Emfret (Würzburg, Germany). Anti–β3 integrin [pY773] phospho-specific antibody was from Biosource International (Camarillo, CA), antimyosin RLC was from Santa Cruz (Santa Cruz, CA), and the enhanced chemiluminescence (ECL) kit was from Amersham Pharmacia Biotech (Orsay, France). Phalloidin–Alexa Fluor 488 and goat anti–rabbit–Alexa Fluor 488 antibody were from Invitrogen, (Cergy Pontoise, France). Complete protease inhibitor cocktail was from Roche Diagnostics (Meylan, France).

Generation of megakaryocyte-restricted MYH9Δ mice

The construction of floxed embryonic stem (ES) cells is detailed in Figure S1 (available on the *Blood* website; see the Supplemental Materials link at the top of the online article). Floxed heterozygous mice (50% C57BL/6-50% 129sv) were crossed with transgenic mice selectively expressing cre-recombinase in the megakaryocyte lineage, under control of the bacterial artificial chromosome (BAC) platelet factor 4 (PF4) promoter (100% C57BL/6).[33] Mice expressing cre gene and heterozygous for the *MYH9* recombination were intercrossed to obtain littermate mice homozygous for the wild-type (wt) *MYH9* allele (+/+ mice) and homozygous for the recombined allele (*MYH9*Δ or −/− mice) or heterozygotes (+/− mice).

Bleeding time

Male and female mice (20-25g) were anesthetized by inhalation of isoflurane. The extremity of the mouse tail was cut transversally with a scalpel (3 mm) and immediately immersed in 0.9% isotonic saline at 37°C. The bleeding time was defined as the time required for arrest of bleeding, and when necessary bleeding was stopped manually at the 10-minute time point to prevent death.

Clot retraction

Citrated platelet-rich plasma (cPRP; adjusted to 300×10^9 platelets/L, 300 μL) obtained by centrifugation of whole blood at 250*g* for 10 minutes was stimulated with thrombin (10 U/mL) in the presence of $CaCl_2$ (20 mM) and incubated at 37°C for up to 5 hours, together with 2 μL of erythrocytes to enhance the contrast of the clot.

Platelet survival

Platelet survival time was determined using a modified method adapted from Peng et al[34] by in vivo biotinylation of platelets through intravenous injection of sulfo-NHS-biotin (2 mg/kg twice with 30-minute interval, 5 mice of each genotype). Biotinylated platelets were counted daily for 4 days at 7-hour intervals. The percentage of biotinylated platelets was determined using flow cytometry by double labeling of whole blood with streptavidin-PE (100 μg/mL) and anti-CD41/CD61-PE.

Platelet activation studies

Blood was drawn from the abdominal aorta, platelets were washed, and aggregation was performed as described.[35] Platelet shape change was visualized by the decrease in light transmission in the absence of fibrinogen and in the presence of eptifibatid (40 μg/mL) to prevent aggregation. Dense granule release was evaluated by the measure of serotonin secretion in platelets loaded with [^{3}H]-5HT. In some cases, platelets were pretreated with blebbistatin (100 μM) for 30 minutes. Static adhesion assays were performed as previously described.[36] Briefly, coverslips were coated with fibrinogen (100 μg/mL), blocked with BSA (5 mg/mL), and washed. Platelet suspensions (20×10^9 platelets/L) were stimulated with thrombin (1 U/mL), immediately plated onto the coverslips, and incubated at 37°C for 45 minutes.

Immunofluorescence

Paraformaldehyde (2%) fixed platelets were permeabilized with 0.05% saponin in the presence of 0.2% bovine serum albumin and incubated with phalloidin–AF 488 or a primary antibody (anti–NMHC-IIA, dilution 1:500) followed by a secondary antibody (goat anti–rabbit AF 488). Cells were embedded in Moviol for confocal observation (confocal microscope TCS SP5, Leica Microsystems, Rueil-Malmaison, France) with oil objectif (100×/1.30 NA). Acquisition software was LAS AF version 1.62 (Leica). Surface area was quantified using Methamorph software (Version 5; Universal Imaging, Downingtown, PA).

Flow cytometry

The activation state of the integrin αIIbβ3 was measured in washed platelets stimulated for 10 minutes with either collagen (100 μg/mL) or thrombin (1 U/mL) without stirring, followed by labeling with Jon/A-PE (1:20)[37]or FITC-labeled antifibrinogen antibody (1:20). The extent of integrin activation was determined for both antibodies by the geometric mean of the relative fluorescence intensity of the whole platelet population (in arbitrary units).

Western blotting

Frozen ground tissue lysates were prepared in 1% Triton X100 buffer. Platelet lysates were prepared by resuspending washed platelets (300×10^9/L), activated or not by thrombin (1 U/mL) for various times, in SDS buffer (1% SDS final concentration). Proteins were separated by sodium dodecyl sulfate–polyacrylamide gel electrophoresis (SDS-PAGE) under reducing conditions, transferred to PVDF membranes, and incubated with the primary antibody (antibody directed against NMHC-IIA, RLC, actin, β3 integrin, or phosphorylated β3 integrin). Quantification was performed using the ImageQuant TL software v2003.03 (Amersham Biosciences). The

amount of phosphorylated β3 integrin was normalized against total β3 integrin, and the NMHC-IIA was normalized against actin.

Lipid extraction and analysis

Platelets were labeled with 0.6 Ci/mL [^{32}P] orthophosphate during 45 minutes in a phosphate-free washing buffer (pH 6.5)[38] at 37°C, washed once, and suspended at a final concentration of 500×10^9 platelets/L (pH 7.38). After stimulation, reactions were stopped by addition of chloroform/methanol (1:1, vol/vol) containing 0.4 N HCl, and lipids were immediately extracted and quantified as described.[38]

Electron microscopy

Platelets were fixed directly in the aggregometer cuvette with 2.5% glutaraldehyde in 0.1 M cacodylate buffer (pH 7.2) containing 2% sucrose. Cells for transmission electron microscopy (TEM) were processed as described previously,[35] and ultrathin sections were examined under a Philips CM120 Biotwin electron microscope (FEI, Eindhoven, The Netherlands) at 120 kV. Scanning electron microscopy (SEM) was performed as described elsewhere[37] under a Sirion scanning electron microscope (FEI) at 5 kV.

In vitro model of thrombosis on immobilized collagen under flow conditions

Platelet thrombus formation was studied as described previously.[39] Control wt mice were injected intraperitoneally with busulfan (30 mg/kg) 14 days before drawing blood so as to obtain a thrombocytopenia ranging from 100×10^9 to 300×10^9 platelets/L. *MYH9*Δ mice were injected with vehicle (polyethylene-glycol). Hirudin-anticoagulated whole blood was perfused through collagen-coated glass capillaries at a shear rate of 3000 s^{-1}. For SEM analysis, the capillaries were rinsed with saline after blood perfusion for 2 minutes and the surface was fixed with 2.5% glutaraldehyde in 0.1 M cacodylate buffer (pH 7.2). The capillaries were sectioned longitudinally, treated, and examined as described previously.[39]

$FeCl_3$-induced carotid artery thrombosis

Carotid artery injury was performed by topical application of $FeCl_3$ for 2 minutes (Whatmann paper 1×0.5 mm soaked with 0.2 μL of 7.5% $FeCl_3$). The artery was then rinsed with saline and the thrombus growth was monitored for 20 minutes. $DIOC_6$ (5 μL of a 100 μM solution/g of body weight) was injected into the jugular vein prior to injury to allow visualization of the thrombus surface. The carotid was placed under a fluorescent macroscope (Macrofluo, objective 5.0×/0.5 NA, Leica Microsystems) for video recording of thrombosis.[40] Fluorescent images were acquired sequentially (1 image/s) using a CoolSNAP EZ camera (Roper Scientific, Evry, France) controlled by Metaview software version 6.3r7 (Universal Imaging). Quantification of embolism was performed using Metamorph software version 5. A region of interest was delineated downstream of the thrombus. Emboli surfaces were expressed as the total number of fluorescent pixels inside the region of interest, measured at each time point.

Statistics

The results are expressed as mean plus or minus SEM. The significance of the differences between genotypes was evaluated using Student *t* test or Student paired *t* test, as mentioned.

Results

Generation of megakaryocyte-specific *MYH9*Δ mice

In order to generate a viable animal model with NMHC-IIA deficiency in the megakaryocytic lineage, we ablated exon 1 from the *MYH9* gene using a *PF4* promoter–driven Cre-loxP system. Exon 1 was excised in vivo (*MYH9*Δ) by crossing *MYH9*$^{Flx/Flx}$ mice with transgenic animals expressing cre-recombinase specifically in megakaryocytes under the control of the *PF4* promoter.[33] *MYH9*$^{Flx/wt}$; *PF4-cre* mice were intercrossed to produce platelet-specific NMHC-IIA–deficient mice (Figure 1A; Document S1), which were obtained in a mendelian ratio and were healthy, with no gross abnormality.

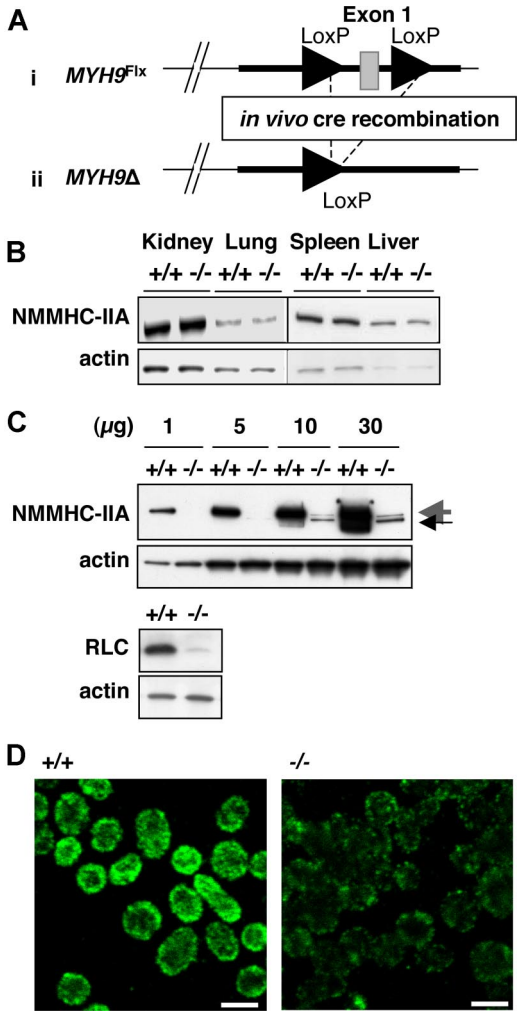

Figure 1. Generation of a platelet-specific *MYH9* knock-down mouse strain exhibiting myosin deficiency. (A) ES cells recombined with the floxed allele were injected into blastocysts to produce chimeric floxed mice (i). Deletion of the *MYH9* exon 1 (*MYH9*Δ) was obtained by exposing the floxed allele to in vivo cre-recombinase expression (ii). (B) Western blot showing NMCH-IIA expression in several tissues from *MYH9*Δ mice (−/−) and control mice (+/+). An identical amount of protein lysate for control or *MYH9*Δ platelets was loaded in each lane, as shown by the similar levels of actin. (C, top panel) Western blot performed with increasing amounts of lysate from control (+/+) and *MYH9*Δ (−/−) platelets (numbers indicate the amount in μg of protein loaded on the gel), showing the residual myosin expressed in platelets (large gray arrow) and exon 1–deleted myosin (small black arrow). (Bottom panel) Western blot showing the regulatory light chain (RLC) expression in control and *MYH9*Δ platelets. (D) The entire population of platelets displayed decreased myosin content in *MYH9*Δ, as revealed by confocal immunofluorescence microscopy (1 image representative of 3 independent mice; bars, 2 μm).

*MYH9*Δ mice exhibit severe NMHC-IIA deficiency

To determine the extent and tissue specificity of the NMHC-IIA deficiency, lysates from platelets and several tissues were analyzed by Western blotting. Normal myosin content was detected in kidney, lung, liver, and spleen of *MYH9*Δ mice (Figure 1B). In contrast, a severe myosin deficiency was found in platelets where the residual myosin amounted to less than 3% of control platelets (Figure 1C top panel).

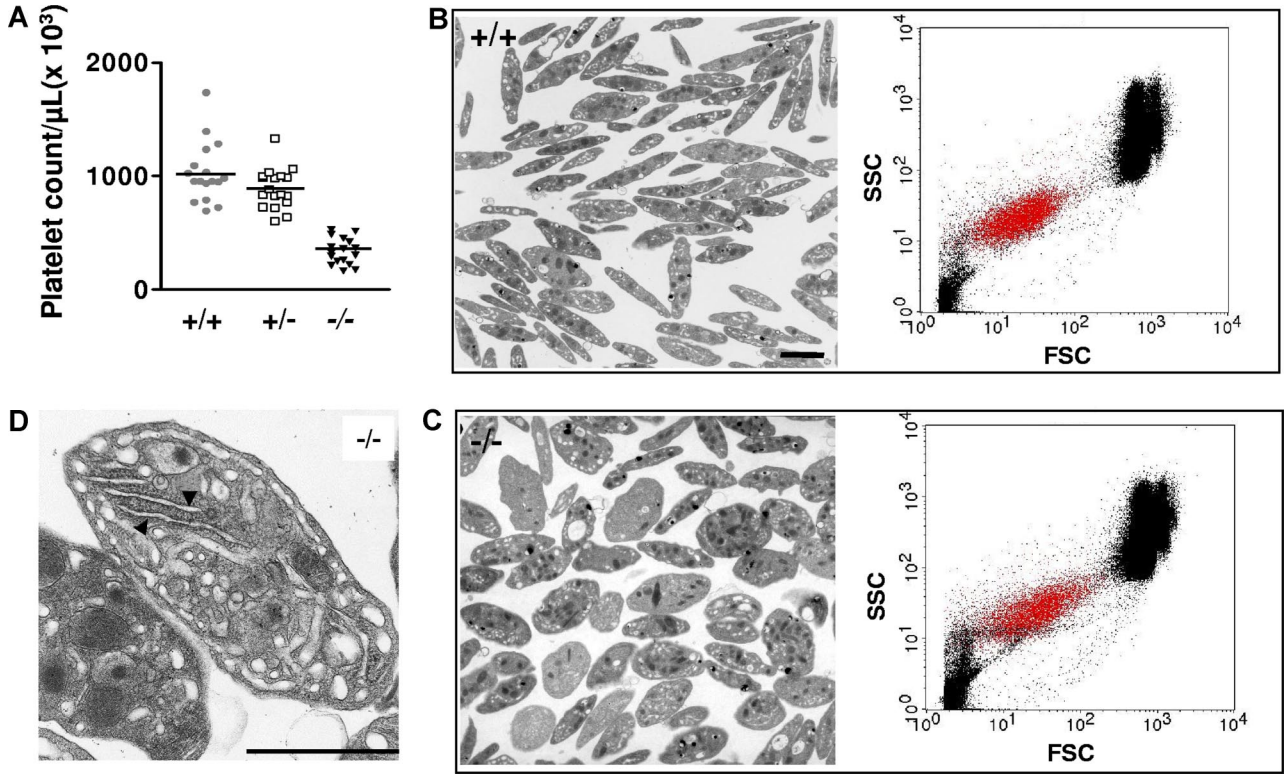

Figure 2. Platelet counts and ultrastructure. (A) *MYH9*Δ mice exhibited thrombocytopenia. The mean is represented in the figure (n = 17-18). (B,C) Heterogeneity in platelet size as observed both by TEM (left panels) and by flow cytometry (right panels, showing representative dot plots of whole blood; FSC indicates forward scatter; SSC, side scatter; $\alpha_{IIb}\beta_3$-positive platelets are visualized by red dots). Control (B) and *MYH9*Δ (C) mouse platelets (bars 2 μm). (D) Higher magnification of a *MYH9*Δ platelet showing the highly developed RER (bar 2 μm).

The antimyosin antibody directed against the C-terminal part of the protein indicated that disruption of the first exon suppressed synthesis of most of the entire protein. A band of slightly lower molecular mass was also observed in *MYH9*Δ platelets only. This band could correspond to residual NMHC-IIA deleted from exon 1, since it is not observed in control platelets. The myosin regulatory light-chain content was likewise considerably decreased in *MYH9*Δ platelets, probably due to its instability in the absence of NMHC-IIA (Figure 1C bottom panel).[41,42] Platelet expression of the residual NMHC-IIA was visualized by immunofluorescence microscopy. As seen in Figure 1D, the intensity of NMHC-IIA labeling was considerably reduced in all *MYH9*Δ platelets compared with control.

*MYH9*Δ mice display thrombocytopenia and altered platelet morphology

Mice deficient in NMHC-IIA reproduced some of the characteristic features of *MYH9*-related diseases in humans. These mice exhibited thrombocytopenia with an average platelet count representing around 40% of wild-type (wt: $1028 \pm 63 \times 10^9$ platelets/L; heterozygous: $890 \pm 41 \times 10^9$ platelets/L; *MYH9*Δ: $336 \pm 28 \times 10^9$ platelets/L; Figure 2A). The decreased platelet count in heterozygote mice was not statistically different compared with wt. These mice also presented an altered platelet morphology with a mean size around twice that of controls as determined by TEM performed on buffy coats (platelet area: 1.8 ± 0.1 [n = 215] vs 4.4 ± 0.2 μm^2 [n = 190] for control and *MYH9*Δ platelets, respectively; $P < .001$, unpaired *t* test) or by whole-blood flow cytometry (forward scatter [FSC] geometric mean of $\alpha_{IIb}\beta_3$-positive population: 15.1 ± 1.3 for control mice vs 26.8 ± 0.9 for *MYH9*Δ mice, n = 5; $P < .001$, unpaired *t* test; Figure 2B-C). Ultrastructural analysis of *MYH9*Δ-washed platelets revealed some heterogeneity with a mixed population of normal discoid and more ovoid morphology compared with the control platelets (Figure 2B,C). A large proportion of these platelets contained large amounts of rough endoplasmic reticulum (RER), typical of young or immature cells as observed both by electron microscopy (15.3% of *MYH9*Δ platelets vs 0.5% of wt platelets, respectively; Figure 2D) and thiazole orange labeling (data not shown). Ultrastructure of platelets from heterozygous animals appeared normal (data not shown). There was no defect in expression of some major platelet glycoproteins ($\alpha_{IIb}\beta_3$, GPIbα, GPIbβ, GPV) as detected by flow cytometry (data not shown).

In vivo platelet half-life was similar in the 2 genotypes (survival time: 112.4 ± 6.1 vs 101.6 ± 4.6 hours for wt and *MYH9*Δ mice, respectively, n = 5; $P > .05$), suggesting that the thrombocytopenia does not result from an accelerated clearance from the circulation and that the increased proportion of reticulated cells mostly reflects a defect in the formation of mature platelets.

*MYH9*Δ mice exhibit a strong increase in bleeding time and a total absence of clot retraction

*MYH9*Δ mice presented no evidence of spontaneous bleeding or hemorrhage. Tail bleeding times were performed to explore primary hemostasis functions following injury. Control wt mice had an average bleeding time of 78 (± 16) seconds (Figure 3A). An increased bleeding time up to 400 seconds was observed in some heterozygous mice, but the average bleeding time was not significantly different from the wt (135 ± 39 s). By contrast, all of the *MYH9*Δ mice bled for more than 600 seconds. It is noteworthy that the bleeding was so important in these mice that they died by 20 minutes unless the wound was manually cauterized (data not shown). By comparison, busulfan-induced thrombocytopenia in wt mice (ranging from 300×10^9 platelets/L to 600×10^9 platelets/L, which is comparable to *MYH9*Δ mice) did not significantly affect the bleeding time (173 ± 24 s; Figure 3A).

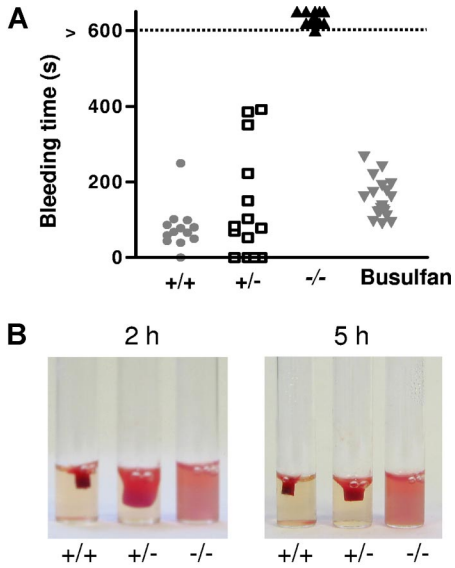

Figure 3. Bleeding time and clot retraction. (A) *MYH9*Δ mice had an increased bleeding time. Points indicate the time required for the arrest of bleeding, and when necessary bleeding was stopped manually after 10 minutes (control wt mice, ●, n = 13; heterozygous mice, □, n = 14; *MYH9*Δ mice, ▼, n = 21; wt mice treated with busulfan to achieve thrombocytopenia comparable to that of *MYH9*Δ mice, ▽, n = 20). (B) Clot retraction was totally abolished in PRP from *MYH9*Δ mice, whereas it was delayed in heterozygous mice. The photograph corresponds to a 2- and 5-hour reaction in cPRP adjusted to 300 × 10^9 platelets/L and treated with 10 U/mL thrombin and is representative of 3 experiments.

Clot retraction, a platelet-dependent contractile phenomenon important for thrombus consolidation, was then investigated. No retraction at all was observed in clots of myosin-deficient platelets 5 hours after thrombin activation, whereas maximal retraction was observed for the wt platelets (Figure 3B). Heterozygous mice exhibited an intermediate phenotype, as the retraction was delayed compared with the wt (Figure 3B).

Thus an intrinsic platelet function defect accounts for this bleeding phenotype independently of the thrombocytopenia.

Platelet aggregation and secretion are barely affected by myosin deficiency

The defective hemostasis in *MYH9*Δ mice led us to investigate in vitro platelet aggregation in response to different concentrations of ADP, thrombin, collagen, and U46619. The velocity and amplitude of aggregation were similar in *MYH9*Δ and control platelets except at the lowest concentration of thrombin (0.02 U/mL) and U46619 (0.5 and 0.1 μM), where a decreased aggregation was observed (Figure 4A). The transient decrease in light transmission that reflects platelet spheration (circled in Figure 4A) was absent in *MYH9*Δ cells, whatever the agonist. Release of [^{3}H] serotonin from dense granules was barely decreased in *MYH9*Δ platelets after stimulation with collagen or high concentrations of thrombin but more reduced after activation with U46619 or low concentrations of thrombin (Table 1). Altogether, there appears to be a minor impact if any of myosin deficiency on platelet aggregation and secretion in suspension. In order to assess whether the residual myosin expression could play a part in the near-normal aggregation and secretion observed, platelets were pretreated with blebbistatin (100 μM), an inhibitor of nonmuscle myosin II activity.[43,44] Under these conditions, blebbistatin totally prevented initial platelet shape change in control platelets. However, no further inhibition of platelet aggregation or secretion was observed in *MYH9*Δ platelets

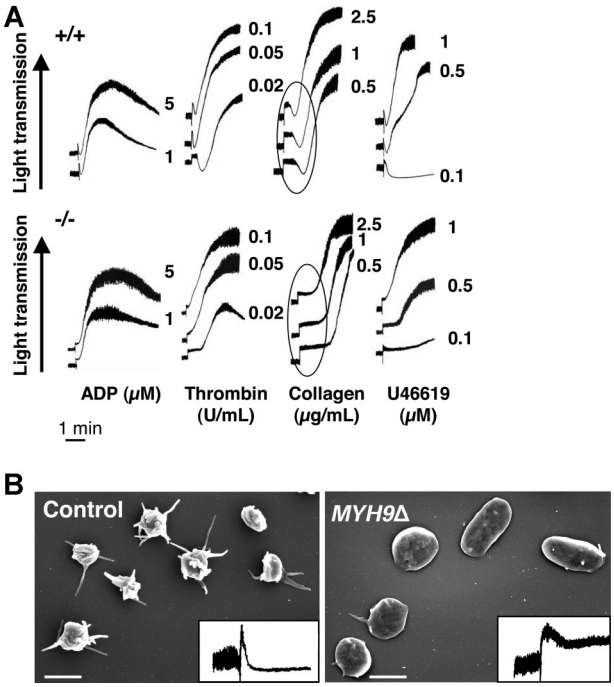

Figure 4. Platelet aggregation is preserved in *MYH9*Δ mice despite absence of initial shape change. (A) Platelet aggregation in response to ADP, thrombin, collagen, and U46619 was barely impaired in *MYH9*Δ mice (numbers correspond to the concentration of agonist). The initial platelet contraction responsible for a transient decrease in light transmission (circled) was absent in *MYH9*Δ platelets. Tracings are representative of at least 3 experiments. (B) Shape change was evaluated in the aggregometer after stimulation of washed platelets with 5 μM ADP in the absence of fibrinogen and the presence of eptifibatid. Shape change was visualized by scanning electron microscopy and by the decrease in light transmission (inset), representative of 3 independent experiments (bars 2 μm).

(data not shown). Thus, these data show that myosin does not play a crucial role in these functions.

Myosin-deficient platelets display impaired contractile shape change and stress-fiber formation

Platelet shape change was further investigated in the aggregometer following addition of 5 μM ADP in the absence of fibrinogen and in the presence of the integrin $\alpha_{IIb}\beta_3$ antagonist eptifibatid to prevent platelet aggregation. As shown in Figure 4B, the shape change was almost abolished in *MYH9*Δ compared with control platelets, whereas platelets from heterozygous mice exhibited normal shape change (data not shown). Observation by SEM revealed the presence of 92% discoid platelets with only a few or no membrane extensions, whereas in the control 72% of the platelets underwent rounding and contraction (Figure 4B). Platelets from heterozygous animals behaved similarly to the control platelets (data not shown). Treatment of platelets with blebbistatin abolished rounding and contraction of control platelets by 96% and had no further significant effect on *MYH9*Δ platelets (data not shown).

Table 1. Percentage 5 HT secretion in wt and *MYH9*Δ mice

Agonists	Control, wt	*MYH9*Δ
Thrombin, 1 U/mL	100	84.0 ± 10
Thrombin, 0.03 U/mL	10.7 ± 3.8	1.2 ± 0.91
Collagen, 100 μg/mL	100	93.0 ± 2.5
Collagen, 5 μg/mL	79.7 ± 1.3	62.3 ± 3.8*
U46619, 1 μM	24.0 ± 0.6	2.7 ± 1.3†

Data are means plus or minus SEM of 3 independent experiments.
*$P < .05$, Student paired *t* test.
†$P < .01$, Student paired *t* test.

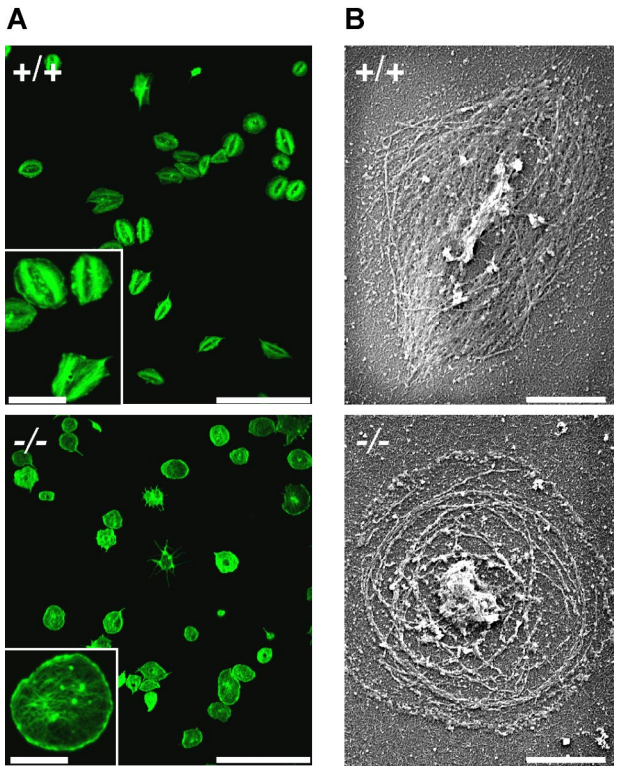

Figure 5. Defective stress-fiber formation during spreading of *MYH9*Δ platelets. Platelets were pretreated with thrombin (1 U/mL) and allowed to adhere to fibrinogen-coated coverslips for 45 minutes. Actin filaments were visualized (A) by confocal fluorescence microscopy after phalloidin-AF 488 labeling (bars 25 μm, inset 7.5 μm) and (B) by SEM after Triton X100 permeabilization (bars 2 μm). Representative of 3 experiments.

Platelet spreading and stress-fiber formation were then studied during adhesion of platelets to a fibrinogen-coated surface. When prestimulated with thrombin, both wt and *MYH9*Δ platelets were able to adhere to the surface and extend lamellipodia, as was revealed by phalloidin labeling of actin fibers (Figure 5A) and SEM after Triton X100 permeabilization (Figure 5B). However, *MYH9*Δ platelets were unable to form stress fiber–like structures contrary to control platelets. Instead, long actin filaments were observed throughout the cytoplasm together with short filaments at the leading edge, and the final mean surface area was increased by 10% (n = 736 and 670 platelets for control and *MYH9*Δ platelets, respectively; $P < .001$ using Student *t* test).

Outside-in signaling is strongly impaired in myosin-deficient platelets

The absence of stress-fiber formation on a fibrinogen matrix together with absent clot retraction prompted us to evaluate signaling through integrin αIIbβ3. Integrin activation was evaluated in control and *MYH9*Δ mice following activation by collagen (100 μg/mL) or thrombin (1 U/mL) in the absence of stirring. The level of activated integrin was measured by flow cytometry using an antibody directed against the activated form of the integrin (Jon/A PE antibody[37]) or against integrin-bound fibrinogen. In both cases, thrombin stimulation led to a significant decrease in αIIbβ3 activation that was not observed with collagen (Figure 6A).

Outside-in signaling was then evaluated by the phosphorylation of the integrin β3 during the course of thrombin-induced platelet aggregation. As shown by immunoblotting, thrombin stimulation led to the phosphorylation of integrin β3 as early as 60 seconds following agonist addition in control platelets. By contrast, in *MYH9*Δ platelets, there was impairment in the phosphorylation of the integrin. By 3 minutes, the amount of integrin β3 phosphorylated in myosin-deficient platelets was decreased by 65% compared with the wt platelets, indicating that myosin plays a role in integrin outside-in signaling (Figure 6B).

To further evaluate defective outside-in signaling, we measured the activity of PI 3-kinase. Particularly, the synthesis of a major part of one of its products, PtdIns(3,4)P_2, is indeed dependent upon the engagement of the integrin.[45,46] The levels of PtdIns(3,4)P_2 and PtdIns(3,4,5)P_3 were measured following platelet stimulation by thrombin or collagen. While the levels of PtdIns(3,4,5)P_2 were comparable between the 2 genotypes (not shown), PtdIns(3,4)P_2 accumulation was reduced by 70% in *MYH9*Δ platelets (Figure 6C), consistent with a defect in outside-in signaling.

Thrombus organization is impaired in vitro under flow conditions and in vivo

To evaluate the role of myosin in the process of thrombus formation, we first investigated thrombus growth in vitro in a

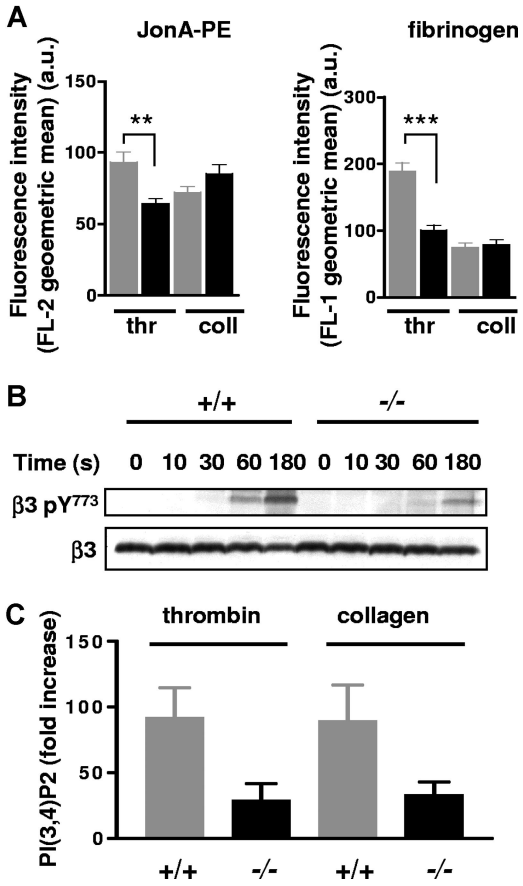

Figure 6. αIIbβ3 integrin activation and outside-in signaling in *MYH9*Δ platelets. (A) Flow-cytometry experiments showing integrin $\alpha_{IIb}\beta_3$ activation as revealed by Jon/A-PE (left panel) or fibrinogen (right panel) labeling following platelet activation by thrombin (thr, 1 U/mL) or collagen (coll, 100 μg/mL) in the absence of agitation. The amount of activated integrin is indicated by the geometric mean of the relative fluorescence intensity, in arbitrary units. Gray and black bars represent control and *MYH9*Δ platelets, respectively; mean (± SEM) n = 3 experiments. (B) Western blots showing phosphorylation of integrin β3 at Y773 (top panel) during stimulation of platelet suspension by thrombin (1 U/mL) for up to 3 minutes in the aggregometer. Identical protein loading was checked by reblotting with an anti-β3 antibody (bottom panel). Blots are representative of 2 experiments. (C) PtdIns(3,4)P_2 synthesis following thrombin (1 U/mL) or collagen (10 μg/mL) stimulation upon 2 minutes. Values have been normalized against total polyphosphoinositides and the results are presented as fold increase compared with nonstimulated platelets (± SEM, n = 3 independent experiments).

whole-blood perfusion assay over a fibrillar collagen matrix under arterial shear-rate conditions (3000 s^{-1}).[47] Keeping in mind the decreased platelet count in *MYH9*Δ mice, wt mice were treated with busulfan to reach thrombocytopenia levels comparable to that of *MYH9*Δ mice ($290 \pm 115 \times 10^9$ platelets/L for busulfan-treated mice, and $220 \pm 103 \times 10^9$ platelets/L for *MYH9*Δ mice). After 2-minute perfusion, analysis of the flow chamber by SEM revealed that the structure of the thrombi was totally different between the genotypes. In the control condition, the compact aggregates formed were composed of contracted platelets tightly packed together. In contrast, aggregates of *MYH9*Δ blood contained only a few layers of platelets that did not have contracted bodies, were rather flat with spread morphology, and were loosely packed compared with the control cells (Figure 7A).

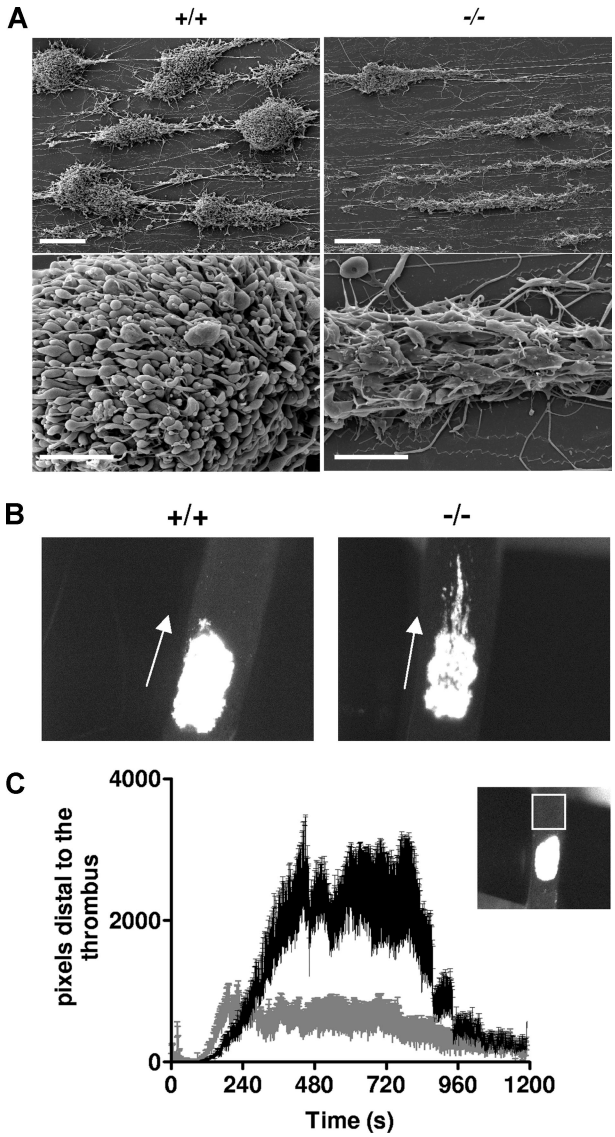

Figure 7. Defective thrombus formation in vitro and in vivo. (A) Whole blood from busulfan-treated wt mice (+/+) or *MYH9*Δ mice (−/−) was anticoagulated with hirudin (100 U/mL) and perfused through collagen-coated glass capillaries at a shear rate of 3000 s^{-1}. Scanning electron microscopy imaging was performed after 2-minute perfusion and images are representative of 3 experiments. Bars, 20 μm (top panels) and 5 μm (bottom panels). (B) $FeCl_3$-induced injury was performed in the carotid of busulfan-treated wt mice (+/+) or *MYH9*Δ mice (−/−) and the thrombus growth was video recorded. Images are representative of 8 mice, at time 600 seconds following injury (original magnification × 45). (C) Time courses of the embolus surface area measured by the fluorescence passing through the region of interest (white square in the insert), downstream of the thrombus. Busulfan-treated wt mice (gray curve) and *MYH9*Δ mice (black curve); n = 8, $P < .001$ (Student paired *t* test).

The capacity of *MYH9*Δ mice to develop a thrombus was then evaluated in vivo in a carotid artery thrombosis model where injury was induced by topical application of $FeCl_3$ and visualized by intravital microscopy[40] (Figure 7B; Videos S1,S2). Busulfan-treated wt mice were used as control. These mice exhibited a platelet count of 312 (± 57) × 10^9 platelets/L (n = 8) similar to platelet counts in *MYH9*Δ mice used in this experiment ($317 \pm 76 \times 10^9$ platelets/L). In control mice, the thrombus was compact and occupied the whole injured surface, as judged by the uniform intensity of fluorescence. By contrast, in *MYH9*Δ mice, the injured surface was not uniformly covered, as observed by the lack of homogeneity of the fluorescence, indicating that platelets were not tightly packed and that the thrombus did not grow in height (Figure 7B; Videos S1,S2). In addition, large emboli were continuously detaching from the thrombus of *MYH9*Δ mice, suggesting instability of the thrombus (Figure 7C).

Discussion

In the present study, we addressed the question of the role of myosin and contractile activity in platelet functions. We established a mouse strain with megakaryocyte-restricted disruption of the *MYH9* gene, leading to severe NMHC-IIA deficiency in platelets amounting to less than 3% of the wt platelets. The reason for the presence of very low amounts of residual myosin could be due to an incomplete excision of the *MYH9* exon 1 by the cre-recombinase in the megakaryocytes. Another possible explanation could be that the residual myosin reflects the long half-life of the NMHC-IIA synthesized before the time where the PF4 promoter becomes functional and promotes the expression of the Cre-recombinase. The appearance in the *MYH9*Δ platelets of a protein with a slightly lower molecular weight indicates that some synthesis from exon 1–deleted mRNA occurs. The presence of this protein in low amounts suggests that either the transcription or the translation is not efficient or that the truncated protein is unstable. In addition, the defect in NMHC-IIA expression led to a decrease in myosin RLC expression. This probably results from instability of the RLC in the absence of the heavy chain as already observed in *Dictyostelium discoideum*[42] and more recently in *Drosophila melanogaster*.[41]

*MYH9*Δ mice presented a platelet phenotype closely resembling that of *MYH9*-related disorders in humans and consisting essentially of thrombocytopenia and large platelets, with an absence of agonist-induced platelet shape change.[18] However, due to its restriction to the megakaryocytic lineage, these mice lack additional defects observed in other tissues in *MYH9*-related diseases. As the defect in protein expression in *MYH9*Δ platelets is more severe than the human defect, *MYH9*Δ mice could represent an interesting model to study some aspects of *MYH9*-related diseases in addition to the role of myosin in platelet functions.

The major observations were that *MYH9*Δ mice exhibited a considerable increase in the bleeding time and total absence of clot retraction. It is unlikely that the thrombocytopenia is the sole reason why *MYH9*Δ mice bled to death upon tail section. Indeed, busulfan-treated wt mice having thrombocytopenia in the same range as *MYH9*Δ mice displayed no such prolongation of the bleeding time. Moreover, in other severely thrombocytopenic mice such as cMpl, β1 tubulin, or GPIbβ knockout mice,[39,48,49] the bleeding tendency was likewise less pronounced. Hence our data suggest that altered platelet functions due to myosin deficiency are responsible for the defects.

The total absence of clot retraction may contribute to increase the bleeding time, since impaired clot retraction has been shown to lead to rebleeding in several mouse models.[50,51] It is noteworthy that defective clot retraction has only been reported in a few *MYH9* patients,[52] and one study mentioned normal clot retraction in a May-Hegglin subject who suffered from bleeding tendency.[53] One may speculate that some myosin activity is preserved in these patients, despite the presence of mutant forms of myosin IIA that are able to interact with the nonmutated counterpart, thus "poisoning" the normal protein.

What makes the observation of increased bleeding time even more puzzling was that in vitro platelet aggregation and secretion were almost unaltered in *MYH9*Δ mice. The very modest impact of myosin deficiency on secretion was unexpected, since early observations that the cytoskeleton directs granule centralization in platelets had long led to the speculation that actomyosin should provide a contractile force facilitating the release of granule contents.[54-56] Furthermore, inhibitors of myosin light-chain kinase or Rho kinase have been shown to block phosphorylation of the myosin light chain, a prerequisite for myosin activation, and to inhibit the release reaction, suggesting that actomyosin contraction is required for granule secretion.[5,12-15] Our results indicate that myosin contraction, while facilitating the release reaction following weak platelet stimulation, is in fact dispensable for platelet secretion when increasing agonist concentrations.

More unexpected, in view of the modest impact on platelet aggregation and secretion, was the alteration in thrombus formation both in vitro under high shear flow and in vivo. The disorganization of the thrombus in myosin-deficient mice is accompanied by an increase in emboli detaching from the thrombi. This effect on thrombus stability is most probably due to a decrease in aggregate stability under high shear forces that could result from both the absence of aggregate compaction and the defect in outside-in signaling. Indeed, aggregate compaction would be expected to allow the thrombus to resist shear forces and also to reduce the space between platelets, thus increasing local concentrations of released agonists. The capacity of platelets to remain in close contact to each other despite the shear forces relies on the engagement of integrins with their ligands, leading to signal transduction that reinforces the interactions between platelets. The αIIbβ3 integrin outside-in signaling resulting from fibrinogen binding leads to tyrosine phosphorylation of several proteins including the β3 subunit itself, activation of the phosphoinositide metabolism, further cytoskeleton reorganization, enhancement of platelet activation, and improved stability of the aggregates.[46,57] Our results show that myosin plays a role in platelet integrin outside-in signaling as observed by a decrease in both PtdIns(3,4)P_2 accumulation and the β3 subunit phosphorylation. Phosphorylation of β3 allows direct interaction of the integrin with myosin. Platelets from DiYF mice, in which β3 cannot be tyrosine phosphorylated, exhibit, like *MYH9*Δ platelets, moderately impaired aggregation and unstable aggregate formation in response to low concentrations of thrombin, together with impaired clot retraction.[51] Thus actomyosin contractility may be important to control the extent of outside-in signaling, maybe through integrin clustering and focal adhesion maturation as is observed in other cells.[58] The way myosin IIA regulates focal adhesion through stress-fiber formation may also contribute to restrict lamellipodia extension in normal platelets following adhesion, similar to migrating cells where loss of NMHC-IIA–based contractility has been shown to relieve a restriction on protrusion extension.[59]

In conclusion, inactivation of *MYH9* in the megakaryocytic lineage results in a severe deficiency in platelet myosin expression with a phenotype that partially resembles *MYH9*-related diseases in humans, including thrombocytopenia and large platelets. On one hand, our results highlight the important role of myosin IIA in outside-in signaling, clot retraction, and thrombus formation and organization, which, in addition to thrombocytopenia, account for the deficient hemostasis observed in *MYH9*Δ mice. On the other hand, myosin plays no major role in platelet aggregation and secretion in suspension. Homozygous gene inactivation obtained in *MYH9*Δ mice differs from the genetic defects resulting from mutations in one *MYH9* allele in patients with *MYH9*-related disorders. In these patients, expression of abnormal myosin is responsible for the pathology. Although this is probably the reason why patients have a less severe hemorrhagic syndrome than mice, the mechanisms described here nevertheless may explain part of the defects of hemostasis observed in the patients.

Acknowledgments

We thank Bernard Payrastre for critical reading of the manuscript. We thank Dominique Cassel, Patricia Laeuffer, Stéphanie Magnenat, Fabienne Proamer, Jean-Yves Rinckel, and Catherine Meyer for expert technical assistance and J. N. Mulvihill for reviewing the English of the manuscript.

This study was supported by ARMESA (Association de Recherche et Développement en Médecine et Santé Publique) and Fondation de France (2007001964). C.L. and B.H. are supported by a "contrat d'interface" between Etablissement Français du sang and Institut National de la Santé et de la Recherche Médicale.

Authorship

Contribution: C.L. designed and performed research, analyzed data, and wrote the paper. A.E. performed and analyzed electron microscopy imaging. B.H., M.J., and C.N. performed and analyzed in vitro thrombus formation and in vivo experimental thrombosis. C.R. and B.A. designed and analyzed flow-cytometry experiments. M.F. took care of the animals and performed animal experimentation. J.W. constructed *MYH9* knockout mice. M.-P.G. and S.S. performed and analyzed phospholipid measurements. R.T. and R.S. contributed PF4-cre mice. J.-P.C. discussed results. F.L. discussed results and wrote the paper. C.G. designed research, analyzed the data, and wrote the paper.

Conflict-of-interest disclosure: The authors declare no competing financial interests.

Correspondence: C. Léon or C. Gachet, INSERM U.311, Etablissement Français du Sang-Alsace (EFS-Alsace), 10 rue Spielmann, B.P. N° 36, 67065 Strasbourg Cedex, France; e-mail: catherine.leon@efs-alsace.fr or christian.gachet@efs-alsace.fr.

References

1. Barkalow KL, Falet H, Hartwig JH. Dynamics of the platelet cytoskeleton. In: Gresele P, Page C, Fuster V, Vermylen J, eds. Platelets in Thrombotic and Non-thrombotic Disorders. Cambridge, United Kingdom: Cambridge University Press; 2002:93-103.
2. Gear ARL, Polanowska-Grabowska Rk. The platelet shape change. In: Gresele P, Page C, Fuster V, Vermylen J, eds. Platelets in Thrombotic and Non-thrombotic Disorders. Cambridge, United Kingdom: Cambridge University Press; 2002:319-337.

3. Fox JE. The platelet cytoskeleton. Thromb Haemost. 1993;70:884-893.
4. Fox JE. Cytoskeletal proteins and platelet signaling. Thromb Haemost. 2001;86:198-213.
5. Suzuki Y, Yamamoto M, Wada H, et al. Agonist-induced regulation of myosin phosphatase activity in human platelets through activation of Rho-kinase. Blood. 1999;93:3408-3417.
6. Paul BZ, Daniel JL, Kunapuli SP. Platelet shape change is mediated by both calcium-dependent and -independent signaling pathways: role of p160 Rho-associated coiled-coil-containing protein kinase in platelet shape change. J Biol Chem. 1999;274:28293-28300.
7. Bauer M, Retzer M, Wilde JI, et al. Dichotomous regulation of myosin phosphorylation and shape change by Rho-kinase and calcium in intact human platelets. Blood. 1999;94:1665-1672.
8. Klages B, Brandt U, Simon MI, Schultz G, Offermanns S. Activation of G12/G13 results in shape change and Rho/Rho-kinase-mediated myosin light chain phosphorylation in mouse platelets. J Cell Biol. 1999;144:745-754.
9. Daniel JL, Molish IR, Rigmaiden M, Stewart G. Evidence for a role of myosin phosphorylation in the initiation of the platelet shape change response. J Biol Chem. 1984;259:9826-9831.
10. Nachmias VT, Kavaler J, Jacubowitz S. Reversible association of myosin with the platelet cytoskeleton. Nature. 1985;313:70-72.
11. Tanaka K, Itoh K. Reorganization of stress fiber-like structures in spreading platelets during surface activation. J Struct Biol. 1998;124:13-41.
12. Lokeshwar VB, Bourguignon LY. The involvement of Ca2+ and myosin light chain kinase in collagen-induced platelet activation. Cell Biol Int Rep. 1992;16:883-897.
13. Nishikawa M, Tanaka T, Hidaka H. Ca2+-calmodulin-dependent phosphorylation and platelet secretion. Nature. 1980;287:863-865.
14. Saitoh M, Naka M, Hidaka H. The modulatory role of myosin light chain phosphorylation in human platelet activation. Biochem Biophys Res Commun. 1986;140:280-287.
15. Watanabe Y, Ito M, Kataoka Y, et al. Protein kinase C-catalyzed phosphorylation of an inhibitory phosphoprotein of myosin phosphatase is involved in human platelet secretion. Blood. 2001; 97:3798-3805.
16. Suzuki-Inoue K, Hughes CE, Inoue O, et al. Involvement of Src kinases and PLCgamma2 in clot retraction. Thromb Res. 2007;120:251-258.
17. Berg JS, Powell BC, Cheney RE. A millennial myosin census. Mol Biol Cell. 2001;12:780-794.
18. Noris P, Spedini P, Belletti S, Magrini U, Balduini CL. Thrombocytopenia, giant platelets, and leukocyte inclusion bodies (May-Hegglin anomaly): clinical and laboratory findings. Am J Med. 1998; 104:355-360.
19. Seri M, Cusano R, Gangarossa S, et al. Mutations in MYH9 result in the May-Hegglin anomaly, and Fechtner and Sebastian syndromes: The May-Hegglin/Fechtner Syndrome Consortium. Nat Genet. 2000;26:103-105.
20. Heath KE, Campos-Barros A, Toren A, et al. Nonmuscle myosin heavy chain IIA mutations define a spectrum of autosomal dominant macrothrombocytopenias: May-Hegglin anomaly and Fechtner, Sebastian, Epstein, and Alport-like syndromes. Am J Hum Genet. 2001;69:1033-1045.
21. Kunishima S, Matsushita T, Kojima T, et al. Immunofluorescence analysis of neutrophil nonmuscle myosin heavy chain-A in MYH9 disorders: association of subcellular localization with MYH9 mutations. Lab Invest. 2003;83:115-122.
22. Pujol-Moix N, Kelley MJ, Hernandez A, Muniz-Diaz E, Espanol I. Ultrastructural analysis of granulocyte inclusions in genetically confirmed MYH9-related disorders. Haematologica. 2004; 89:330-337.
23. Canobbio I, Noris P, Pecci A, Balduini A, Balduini CL, Torti M. Altered cytoskeleton organization in platelets from patients with MYH9-related disease. J Thromb Haemost. 2005;3:1026-1035.
24. Heynen MJ, Blockmans D, Verwilghen RL, Vermylen J. Congenital macrothrombocytopenia, leucocyte inclusions, deafness and proteinuria: functional and electron microscopic observations on platelets and megakaryocytes. Br J Haematol. 1988;70:441-448.
25. Lusher JM, Barnhart MI. Congenital disorders affecting platelets. Semin Thromb Hemost. 1977; 4:123-186.
26. Jantunen E. Inherited giant platelet disorders. Eur J Haematol. 1994;53:191-196.
27. D'Apolito M, Guarnieri V, Boncristiano M, Zelante L, Savoia A. Cloning of the murine non-muscle myosin heavy chain IIA gene ortholog of human MYH9 responsible for May-Hegglin, Sebastian, Fechtner, and Epstein syndromes. Gene. 2002; 286:215-222.
28. Matsushita T, Hayashi H, Kunishima S, et al. Targeted disruption of mouse ortholog of the human MYH9 responsible for macrothrombocytopenia with different organ involvement: hematological, nephrological, and otological studies of heterozygous KO mice. Biochem Biophys Res Commun. 2004;325:1163-1171.
29. Franke JD, Dong F, Rickoll WL, Kelley MJ, Kiehart DP. Rod mutations associated with MYH9-related disorders disrupt nonmuscle myosin-IIA assembly. Blood. 2005;105:161-169.
30. Deutsch S, Rideau A, Bochaton-Piallat ML, et al. Asp1424Asn MYH9 mutation results in an unstable protein responsible for the phenotypes in May-Hegglin anomaly/Fechtner syndrome. Blood. 2003;102:529-534.
31. Pecci A, Noris P, Invernizzi R, et al. Immunocytochemistry for the heavy chain of the non-muscle myosin IIA as a diagnostic tool for MYH9-related disorders. Br J Haematol. 2002;117:164-167.
32. Conti MA, Even-Ram S, Liu C, Yamada KM, Adelstein RS. Defects in cell adhesion and the visceral endoderm following ablation of nonmuscle myosin heavy chain II-A in mice. J Biol Chem. 2004;279:41263-41266.
33. Tiedt R, Schomber T, Hao-Shen H, Skoda RC. Pf4-Cre transgenic mice allow generating lineage-restricted gene knockouts for studying megakaryocyte and platelet function in vivo. Blood. 2007;109:1503-1506.
34. Peng J, Friese P, Heilmann E, George JN, Burstein SA, Dale GL. Aged platelets have an impaired response to thrombin as quantitated by P-selectin expression. Blood. 1994;83:161-166.
35. Leon C, Hechler B, Freund M, et al. Defective platelet aggregation and increased resistance to thrombosis in purinergic P2Y(1) receptor-null mice. J Clin Invest. 1999;104:1731-1737.
36. McCarty OJ, Larson MK, Auger JM, et al. Rac1 is essential for platelet lamellipodia formation and aggregate stability under flow. J Biol Chem. 2005; 280:39474-39484.
37. Kauffenstein G, Bergmeier W, Eckly A, et al. The P2Y(12) receptor induces platelet aggregation through weak activation of the alpha(IIb)beta(3) integrin: a phosphoinositide 3-kinase-dependent mechanism. FEBS Lett. 2001;505:281-290.
38. Payrastre B. Phosphoinositides: lipid kinases and phosphatases. Methods Mol Biol. 2004;273:201-212.
39. Strassel C, Nonne C, Eckly A, et al. Decreased thrombotic tendency in mouse models of the Bernard-Soulier syndrome. Arterioscler Thromb Vasc Biol. 2007;27:241-247.
40. Gross S, Tilly P, Hentsch D, Vonesch JL, Fabre JE. Vascular wall-produced prostaglandin E2 exacerbates arterial thrombosis and atherothrombosis through platelet EP3 receptors. J Exp Med. 2007;204:311-320.
41. Franke JD, Boury AL, Gerald NJ, Kiehart DP. Native nonmuscle myosin II stability and light chain binding in Drosophila melanogaster. Cell Motil Cytoskeleton. 2006;63:604-622.
42. Knecht DA, Loomis WF. Developmental consequences of the lack of myosin heavy chain in Dictyostelium discoideum. Dev Biol. 1988;128:178-184.
43. Limouze J, Straight AF, Mitchison T, Sellers JR. Specificity of blebbistatin, an inhibitor of myosin II. J Muscle Res Cell Motil. 2004;25:337-341.
44. Straight AF, Cheung A, Limouze J, et al. Dissecting temporal and spatial control of cytokinesis with a myosin II inhibitor. Science. 2003;299: 1743-1747.
45. Guinebault C, Payrastre B, Racaud-Sultan C, et al. Integrin-dependent translocation of phosphoinositide 3-kinase to the cytoskeleton of thrombin-activated platelets involves specific interactions of p85 alpha with actin filaments and focal adhesion kinase. J Cell Biol. 1995;129:831-842.
46. Payrastre B, Missy K, Trumel C, Bodin S, Plantavid M, Chap H. The integrin alpha IIb/beta 3 in human platelet signal transduction. Biochem Pharmacol. 2000;60:1069-1074.
47. Nonne C, Lenain N, Hechler B, et al. Importance of platelet phospholipase Cgamma2 signaling in arterial thrombosis as a function of lesion severity. Arterioscler Thromb Vasc Biol. 2005;25:1293-1298.
48. Bunting S, Widmer R, Lipari T, et al. Normal platelets and megakaryocytes are produced in vivo in the absence of thrombopoietin. Blood. 1997;90: 3423-3429.
49. Schwer HD, Lecine P, Tiwari S, Italiano JE Jr, Hartwig JH, Shivdasani RA. A lineage-restricted and divergent beta-tubulin isoform is essential for the biogenesis, structure and function of blood platelets. Curr Biol. 2001;11:579-586.
50. Goschnick MW, Lau LM, Wee JL, et al. Impaired "outside-in" integrin alphaIIbbeta3 signaling and thrombus stability in TSSC6-deficient mice. Blood. 2006;108:1911-1918.
51. Law DA, DeGuzman FR, Heiser P, Ministri-Madrid K, Killeen N, Phillips DR. Integrin cytoplasmic tyrosine motif is required for outside-in alphaIIb-beta3 signalling and platelet function. Nature. 1999;401:808-811.
52. Godwin HA, Ginsburg AD. May-Hegglin anomaly: a defect in megakaryocyte fragmentation? Br J Haematol. 1974;26:117-128.
53. Volpe E, Cuccurullo L, Valente A, Jori GP, Buonanno G. The May-Hegglin anomaly: further studies on leukocyte inclusions and platelet ultrastructure. Acta Haematol. 1974;52:238-247.
54. Painter RG, Ginsberg MH. Centripetal myosin redistribution in thrombin-stimulated platelets: relationship to platelet Factor 4 secretion. Exp Cell Res. 1984;155:198-212.
55. Gerrard JM, Israels SJ, Friesen LL. Protein phosphorylation and platelet secretion. Nouv Rev Fr Hematol. 1985;27:267-273.
56. White JG, Gerrard JM. Recent advances in platelet structural physiology. Suppl Thromb Haemost. 1978;63:49-60.
57. Phillips DR, Prasad KS, Manganello J, Bao M, Nannizzi-Alaimo L. Integrin tyrosine phosphorylation in platelet signaling. Curr Opin Cell Biol. 2001;13:546-554.
58. Chrzanowska-Wodnicka M, Burridge K. Rho-stimulated contractility drives the formation of stress fibers and focal adhesions. J Cell Biol. 1996;133:1403-1415.
59. Sandquist JC, Swenson KI, Demali KA, Burridge K, Means AR. Rho kinase differentially regulates phosphorylation of nonmuscle myosin II isoforms A and B during cell rounding and migration. J Biol Chem. 2006;281:35873-35883.